iScience

CellPress
OPEN ACCESS

Article

Zhx2 maintains islet β-cell mass and function by transcriptionally regulating Pax6

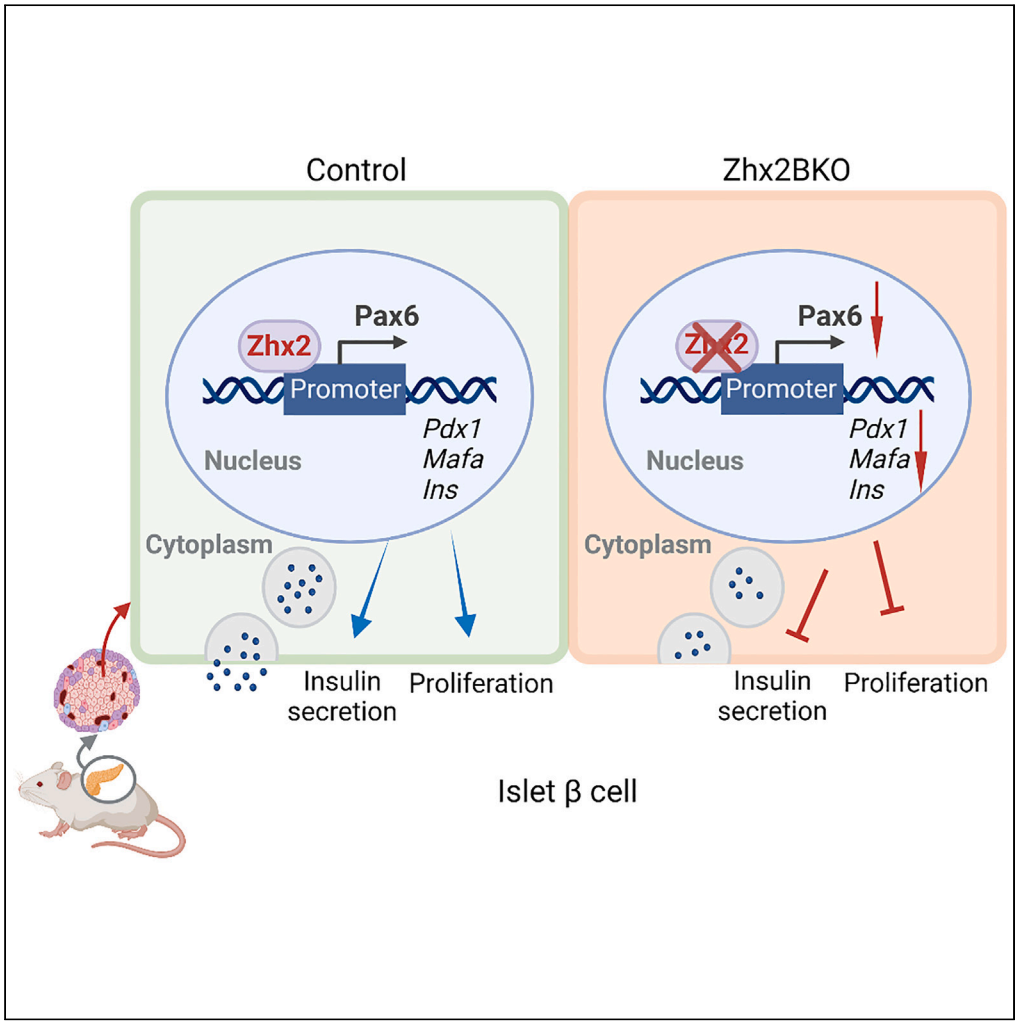

Lu Ding, Yankun Zhang, Yingchun Wang, ..., Xiaohong Liang, Chunhong Ma, Lifen Gao

glfflg@sdu.edu.cn

Highlights

Zhx2 deletion in islet β-cells impairs glucose homeostasis *in vivo*

Zhx2 promotes β-cell proliferation and insulin secretion

Zhx2 maintains β-cell function by transcriptionally regulating Pax6

Ding et al., iScience *26*, 106871
June 16, 2023
https://doi.org/10.1016/j.isci.2023.106871

iScience

CellPress
OPEN ACCESS

Article

Zhx2 maintains islet β-cell mass and function by transcriptionally regulating Pax6

Lu Ding,[1] Yankun Zhang,[1] Yingchun Wang,[1] Yuzhen Wang,[1] Zheng Tong,[1] Pengfei Li,[2] Chaojia Chen,[1] Bo Wang,[1] Xuetian Yue,[3] Chunyang Li,[4] Zhuanchang Wu,[1] Xiaohong Liang,[1] Chunhong Ma,[1] and Lifen Gao[1,5,*]

SUMMARY

Emerging evidence shows that pancreatic β-cell function and quality are key determinants in the progression of type 2 diabetes (T2D). The transcription factor zinc finger homeobox 2 (Zhx2) is involved in proliferation and development of multiple cells. However, the exact role of Zhx2 in β-cells and T2D remains completely unknown. Here, we report that Zhx2 orchestrates β-cell mass and function by regulating paired box protein pax-6 (Pax6). We found that β-cell-specific knockout Zhx2 (Zhx2BKO) mice showed a decrease in β-cell proliferation and glucose homeostasis. Under prediabetic and diabetic conditions, we discovered glucose intolerance in both Zhx2BKO-HFD mice and Zhx2BKO-db/db mice, with reduced β-cell mass and insulin secretion. Mechanistically, we demonstrated that Zhx2 targeted the Pax6 promoter region (−1740∼-1563; −862∼-559; −251∼+75), enhanced promoter activity. Overall, Zhx2 maintains β-cell function by transcriptionally regulating Pax6, which provides a therapeutic target for diabetes intervention.

INTRODUCTION

Type 2 diabetes (T2D), the predominant form of diabetes, has become a global epidemic and is a major risk factor associated with several metabolic syndromes.[1–3] The secretion of insulin from β-cells is exquisitely regulated to meet metabolic demand through complex mechanisms. β-cell dysfunction, responsible for defective insulin secretion and elevated blood glucose levels, represents a key hallmark of T2D.[4] Furthermore, inadequate β-cell mass leads to insulin insufficiency, a contributor to the onset of hyperglycemia in both type 1 diabetes and T2D.[5,6] Therefore, efforts are being made to find potential therapeutic targets for T2D prevention and treatment.

It is well known that β-cells are the source of endogenous insulin, and data from prediabetes, diabetes, and obesity in animal models and humans show that the maintenance of pancreatic β-cell function and mass is a critical determinant of T2D progression.[7–9] The β-cell proliferates compensatively during prediabetes to ensure that relatively normal blood sugar is maintained even in peripheral insulin resistance.[7,10] Thus, key molecules that promote β-cell proliferation and maintain insulin secretion are potentially important in the treatment of T2D.

The zinc fingers and homeoboxes (ZHX) family includes ZHX1, 2, and 3. Zhx2 is located on 8q24. 13 and contains two zinc finger domains and five homeodomains.[11] Evidence shows that Zhx2 regulates cell proliferation.[12–14] Importantly, Zhx2 is also involved in the regulation of the development of a variety of cell types, such as liver cells, nerve cells, red blood cells, and B cells.[15–18] Previously, our group defined Zhx2 as a tumor suppressor in hepatocellular carcinoma for the first time.[13,19] However, Zhx2 emerges as a tumor oncogene in clear cell renal cell carcinoma and breast cancer.[12,14,20] In addition, Zhx2 plays an important role in the regulation of immunocytes and inflammatory diseases, such as restricting NK-cell maturation[21] and promoting macrophage glycolysis and survival in sepsis.[22,23] These data suggest that Zhx2 regulates a variety of cellular functions, particularly cell proliferation and inflammation. T2D is known to be associated with abnormal proliferation of β-cells and chronic inflammation.[24,25] However, the exact role of Zhx2 in T2D remains largely unknown.

The transcription of the insulin gene is strictly regulated by a number of factors, including *MafA*, *Pax6*, and *Pdx1*.[26,27] Among those, Pax6 is a transcription factor crucial for the development of the eye, brain, and

[1]Key Laboratory for Experimental Teratology of Ministry of Education, Shandong Key Laboratory of Infection and Immunity, and Department of Immunology, School of Basic Medical Sciences, Cheeloo College of Medicine, Shandong University, Jinan, Shandong 250012, P. R. China

[2]Department of Endocrinology, Yucheng People's Hospital, Dezhou, Shandong 251200, P. R. China

[3]Department of Cell Biology, School of Basic Medical Sciences, Cheeloo College of Medicine, Shandong University, Jinan, Shandong 250012, P. R. China

[4]Key Laboratory for Experimental Teratology of Ministry of Education and Department of Histology and Embryology, School of Basic Medical Sciences, Cheeloo College of Medicine, Shandong University, Jinan, Shandong 250012, P. R. China

[5]Lead contact

*Correspondence: glfflg@sdu.edu.cn

https://doi.org/10.1016/j.isci.2023.106871

pancreatic islets.[28,29] And Pax6 has been reported to be one of the major factors determining adult β-cell function.[30] Notably, Pax6 has been shown to bind the promoter regions of several key β-cell genes, such as *Slc2a2*, *Pdx1*, *MafA*, *Ins*,[27,31] and Pax6 mutation heterozygosity leads to impaired insulin secretion and subsequent abnormal glucose metabolism in both humans and mice.[30,32] Therefore, Pax6 plays a key role in T2D-associated β-cell dysfunction,[30,33,34] indicating that the factors regulating Pax6 might participate in T2D pathogenesis.

Here, we identified a new role of Zhx2 as a transcriptional regulator of Pax6 in maintaining β-cell mass and function. We found that Zhx2 deficiency in pancreatic islet β-cells led to β-cell loss and dysfunction. Moreover, Zhx2 targeted the Pax6 promoter and promoted Pax6 expression. Eventually, we uncovered a Pax6-dependent mechanism by which Zhx2 deficiency suppresses islet β-cell proliferation and insulin secretion. In conclusion, we demonstrate that Zhx2 regulates β-cell function and quality under normal and prediabetic conditions. Thus, Zhx2, as a previously undescribed regulator of islet β-cells, may represent a novel therapeutic target for T2D intervention.

RESULTS

Zhx2 deletion in islet β-cells impairs glucose homeostasis *in vivo*

We detected Zhx2 expression in different organs of mice by qRT-PCR, and the results showed that Zhx2 was highly expressed in pancreatic islets (Figure S1A). Zhx2 expression in pancreatic islets was confirmed by IHC staining (Figure S1B). Intriguingly, Zhx2 expression in islet β-cells was higher than that in non β-cells (Figures S1C–S1E). Immunofluorescence (IF) staining was performed to further confirm that Zhx2 was highly expressed in insulin-expressing β-cells, compared to α and δ cells (Figure S1F). In addition, we also detected higher mRNA and protein levels of Zhx2 in the β-cell line MIN6 (Figures S1G and S1H). These results demonstrate that Zhx2 is highly expressed in islet β-cells, indicating the potential role of Zhx2 in regulating islet β-cells.

Next, we tried to determine the expression of Zhx2 under high glucose conditions. We detected the mRNA and protein levels in pancreas of 16- to 20-week-old db/m and db/db mice, a model for T2D. The results showed that Zhx2 expression was markedly reduced in the pancreas of db/db mice (Figures S2A–S2C). Zhx2 mRNA was significantly reduced in the islets of db/db mice (Figure S2D). Then, high-fat diet (HFD) combined with streptozotocin (STZ) for 5 months was used to induce T2D in mice.[35] Mice in the STZ + HFD group were fed an HFD diet for 1 month, fasted for 12 h, and intraperitoneally injected with 50 mg/kg STZ for 3 days, followed by HFD-diet feeding for an additional 4 months (Figure S2E). We found that Zhx2 expression was reduced in the islets of mice in the STZ+HFD group (Figure S2F). Consistently, MIN6 cells exposed to high glucose (33.3 mM) for 48 h showed obviously reduced Zhx2 expression (Figures S2G and S2H). We also observed a reduced fluorescence intensity of Zhx2 in islet β-cells of 20-week-old db/db mice (Figure S2I). Taken together, these results illustrate that Zhx2 expression is decreased under diabetic conditions, which might be associated with β-cell failure and diabetes.

The β-cell-specific expression of Zhx2 drove us to investigate whether Zhx2 plays a role in β-cells. To clarify the function of Zhx2 in islet β-cells, we bred Zhx2-floxed ($Zhx2^{f/f}$) mice with RIP-Cre (Ins2-Cre) mice,[36,37] generating mice with conditional *Zhx2* knockout in β-cells, i.e., $Ins2^{Cre+/-}Zhx2^{f/f}$ mice (hereafter referred to as Zhx2BKO) (Figures 1A and S3A). *Ins2* is expressed in both pancreatic islets and the hypothalamus,[38,39] but we observed an extremely low level of Zhx2 protein in the hypothalamus compared to islets (Figures S3B and S3C). Islets and indicated tissues were isolated to detect the knockout efficiency of Zhx2 in islets. qRT-PCR (Figure 1B), Western blotting (Figures 1C and S3D), IF staining (Figure 1D), and IHC staining (Figure S3E) revealed that the levels of Zhx2 mRNA and protein were drastically decreased in the islets of Zhx2BKO mice relative to those of control littermates. Compared to Ins2-Cre mice, the body weight and random glucose showed no significant difference in Zhx2BKO mice, but fasting blood glucose was higher in Zhx2BKO mice (Figures 1E–1G). The fasting blood insulin tended to be lower in Zhx2BKO mice (Figure 1H). Glucose tolerance test (GTT) results revealed that the blood glucose levels were significantly increased in 8- to 12-week-old male Zhx2BKO mice compared with sex- and age-matched Ins2-Cre mice (Figure 1I). We next performed GSIS assays to investigate whether Zhx2 regulates insulin secretion in mice. Compared to Ins2-Cre mice, Zhx2BKO mice did not display an initial burst of insulin secretion within 5 min of glucose injection. The insulin responses were markedly impaired in Zhx2BKO mice compared with control littermates (Figure 1J), although ITT results showed no significant difference in insulin sensitivity between the two groups (Figure 1K). A significant decrease in islet β-cell mass was

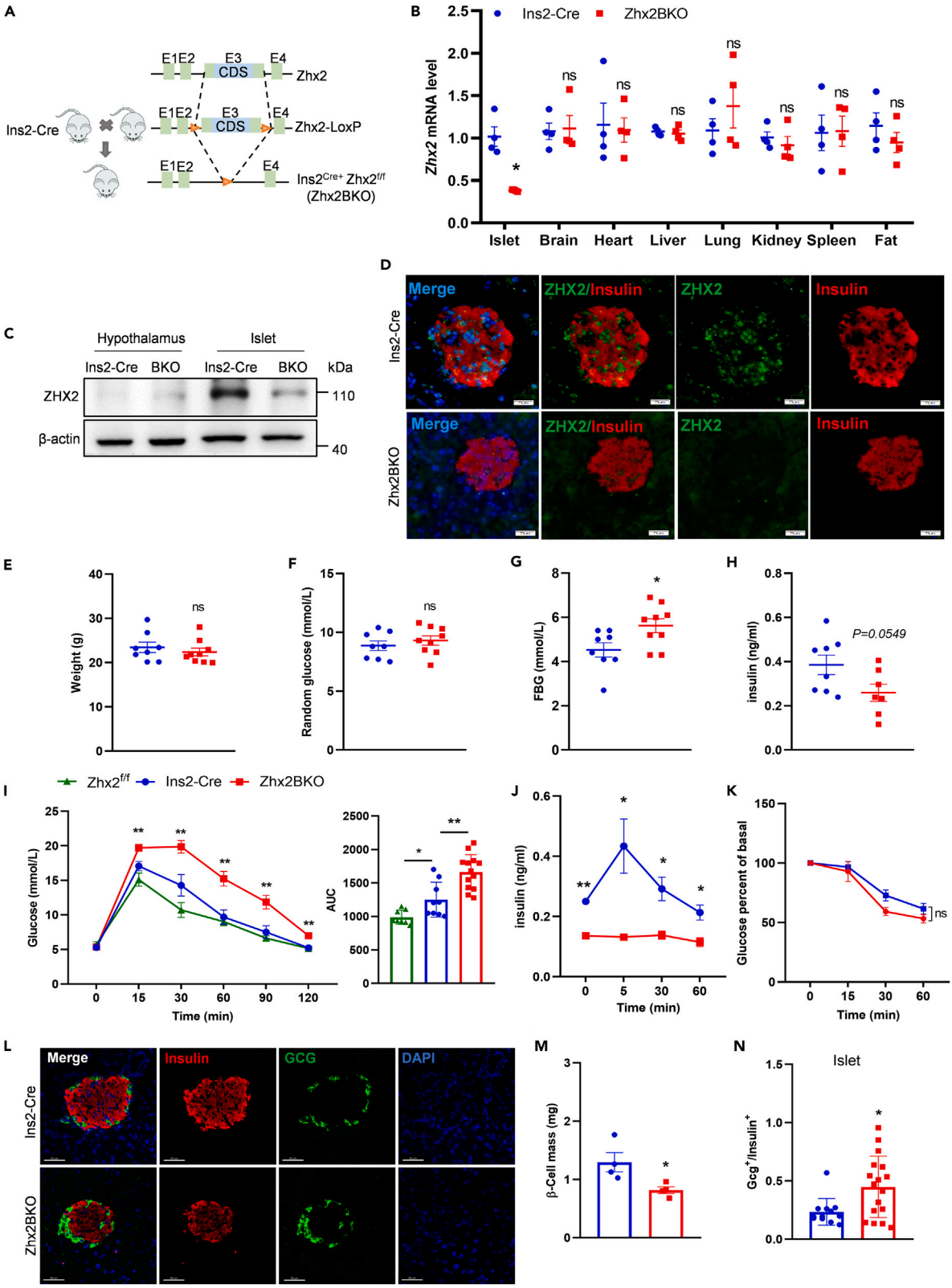
A
E1E2
E3
CDS
E4
Zhx2
Ins2-Cre
Zhx2-LoxP
Ins2Cre+ Zhx2f/f
(Zhx2BKO)
B
Ins2-Cre
Zhx2BKO
Zhx2 mRNA level
ns
*
Islet
Brain
Heart
Liver
Lung
Kidney
Spleen
Fat
C
Hypothalamus
Islet
Ins2-Cre
BKO
kDa
ZHX2
β-actin
110
40
D
Merge
ZHX2/Insulin
ZHX2
Insulin
E
Weight (g)
F
Random glucose (mmol/L)
G
FBG (mmol/L)
H
insulin (ng/ml)
P=0.0549
I
Zhx2f/f
Glucose (mmol/L)
Time (min)
AUC
J
insulin (ng/ml)
Time (min)
K
Glucose percent of basal
Time (min)
L
Merge
Insulin
GCG
DAPI
M
β-Cell mass (mg)
N
Islet
Gcg+/Insulin+

Figure 1. Zhx2 deficiency in β-cells impairs glucose homeostasis

(A) Strategy of islet β-cell-specific Zhx2 knockout mice.

(B) Total RNA isolated from the pancreas of 8- to 12-week-old Ins2-Cre and Zhx2BKO ($Ins2^{Cre+/-}Zhx2^{f/f}$) mice were subjected to qRT-PCR analysis for Zhx2 expression. Zhx2 mRNA was normalized to β-actin mRNA. (n/Ins2-Cre = 4, n/Zhx2BKO = 4).

(C) Protein extracts isolated from hypothalamus and islet tissues of 8- to 12-week-old Ins2-Cre and Zhx2BKO mice were subjected to Western blotting analysis for ZHX2 expression.

(D–H) IF staining of pancreatic sections of Ins2-Cre and Zhx2BKO mice with anti-Zhx2 and anti-insulin antibodies. Scale bar, 50 μm. Body weight (E), random blood glucose level (F), fasting blood glucose level (FBG) (G), and fasting serum insulin level (H) were detected in 3-month-old male Ins2-Cre and Zhx2BKO mice. (n/Ins2-Cre = 8, n/Zhx2BKO = 9). Mice were treated in H (n/Ins2-Cre = 8, n/Zhx2BKO = 7).

(I) Three-month-old male $Zhx2^{f/f}$, Ins2-Cre, and Zhx2BKO mice were fasted for 16 h and intraperitoneally injected with glucose (2 g/kg body weight). Blood glucose levels (left panel) and area under the curve (AUC) (right panel) during the intraperitoneal glucose tolerance test (IPGTT). ($n/Zhx2^{f/f}$ = 8, n/Ins2-Cre = 9, n/Zhx2BKO = 13).

(J) Mice treated as in I and intraperitoneally injected with glucose (2 g/kg body weight). Blood insulin levels were measured by ELISA at 0, 5, 30, and 60 min after glucose injection. (n/Ins2-Cre = 4, n/Zhx2BKO = 3).

(K) Mice fasted for 6 h were intraperitoneally injected with a single dose of recombinant human insulin (0.7 U/kg body weight). The results are expressed as the percentage of the initial blood glucose concentration. (n/Ins2-Cre = 3, n/Zhx2BKO = 4).

(L–N) IF staining was used to detect insulin and GCG (glucagon)-positive α cells in pancreatic sections, followed by measurements of β-cell mass (M) and α/β-cell ratios (islet) (N). (n/Ins2-Cre = 4, n/Zhx2BKO = 4). Data are presented as the mean ± SEM. Data were statistically analyzed by Student's *t* test or two-way ANOVA with Dunnett's post hoc test (K). *$p < 0.05$, **$p < 0.01$, ns indicates no significant difference.

observed in Zhx2BKO mice (Figures 1L and 1M). Accordingly, the α/β-cell ratios were dramatically increased in Zhx2BKO mice compared with the control littermate mice (Figure 1N). Collectively, Zhx2 deficiency in β-cells impairs glucose homeostasis.

Zhx2 deletion leads to a diabetes-like phenotype and reduced β-cell proliferation in T2D mice induced by HFD

HFD-fed mice become obese and prediabetic, as shown by peripheral insulin resistance, moderate hyperglycemia, hyperinsulinemia, and compensatory increase in islet β-cell mass.[7,40] Prolonged (3–6 months) exposure to high lipid concentrations is recommended to induce T2D models and increase β-cell mass by inducing β-cell proliferation.[41,42] Here, we aimed to determine whether HFD stress influenced β-cell function in Zhx2BKO mice during the prediabetic state. We found that HFD feeding did not cause significant weight changes in Zhx2BKO mice compared with Ins2-Cre mice (Figures 2A and 2B). Compared to Ins2-Cre mice, the fasting blood glucose levels were higher in Zhx2BKO mice (Figure 2C), while fasting insulin levels were reduced in Zhx2BKO mice (Figure 2D). We detected GTT of $Zhx2^{f/f}$, Ins2-Cre, and Zhx2BKO mice exposed to an HFD for 3–6 months, and the results showed that Zhx2BKO mice had obvious glucose intolerance compared to control mice (Figure 2E). Consistently, HFD-fed Zhx2BKO mice exhibited reduced insulin secretion in the GSIS test (Figure 2F), but no significant difference was found in insulin resistance compared to the control (Figure 2G). Notably, a significant decrease in the islet area ratio (per whole pancreas) and islet size was observed in the HFD-fed Zhx2BKO mice (Figures 2H–2J). Accordingly, the β-cell area/pancreatic area ratio and β-cell mass were dramatically reduced in Zhx2BKO mice compared with those of the control littermate mice (Figures 2K–2M). IF staining of insulin and the proliferation marker protein Ki-67 (Ki67) revealed that β-cell proliferation was significantly reduced in Zhx2BKO mice compared with the control littermate mice under HFD stress (Figure 2N). In addition, we found that Zhx2BKO mice appeared to have an increased α cell ratio (per islet) compared to Ins2-Cre mice fed a 6-month HFD (Figure S5A). These results verify that Zhx2 deletion leads to reduced β-cell mass, β-cell proliferation, and blood glucose stability under HFD stress, which might contribute to the diabetic phenotype in Zhx2BKO mice.

Zhx2 deficiency promotes β-cell loss and insulin insufficiency in db/db mice

The role of Zhx2 in islet β-cells under T2D conditions was further investigated in Zhx2 knockout db/db mice. Surprisingly, we found that Zhx2 deletion in 16-week-old db/db mice tended to have greater effects (Figure S4A) and led to higher fasting blood glucose levels (Figure S4B), glucose intolerance (Figure S4C), and lower insulin secretion (Figure S4D), while insulin resistance was not significantly altered in Zhx2BKO-db/db mice (Figure S4E). Notably, 16-week-old Zhx2BKO-db/db mice appeared to have a lower islet area ratio (per whole pancreas) and smaller islet size than Ins2-Cre-db/db mice (Figures S4F–S4H). We further measured the β-cell area/islet area ratio of Zhx2BKO-db/db mice, and the results demonstrated that the β-cell area was dramatically reduced in Zhx2BKO-db/db mice compared with the control littermate mice (Figures S4I and S4J). In addition, an increased α cell ratio (per islet) (Figure S5B) was observed in db/db mice lacking Zhx2. Together, Zhx2 deficiency in β-cells of db/db mice accelerates β-cell loss and insulin insufficiency under T2D conditions.

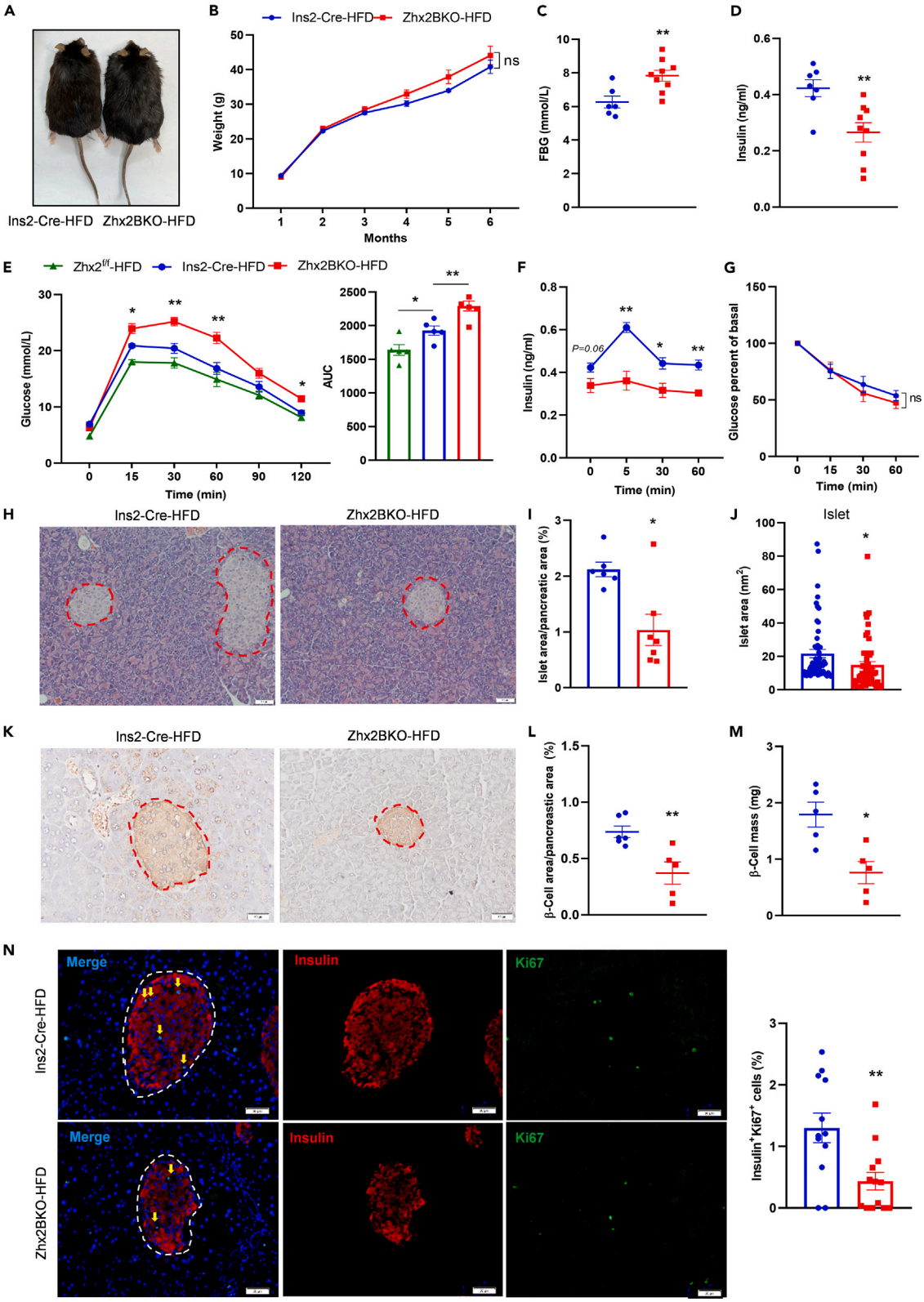
A
Ins2-Cre-HFD Zhx2BKO-HFD
B
Ins2-Cre-HFD Zhx2BKO-HFD
Weight (g)
Months
ns
C
FBG (mmol/L)
D
Insulin (ng/ml)
E
Zhx2f/f-HFD Ins2-Cre-HFD Zhx2BKO-HFD
Glucose (mmol/L)
Time (min)
AUC
F
Insulin (ng/ml)
P=0.06
Time (min)
G
Glucose percent of basal
ns
Time (min)
H
Ins2-Cre-HFD
Zhx2BKO-HFD
I
Islet area/pancreatic area (%)
J
Islet
Islet area (nm2)
K
Ins2-Cre-HFD
Zhx2BKO-HFD
L
β-Cell area/pancreatic area (%)
M
β-Cell mass (mg)
N
Ins2-Cre-HFD
Zhx2BKO-HFD
Merge
Insulin
Ki67
Insulin+Ki67+ cells (%)

Figure 2. HFD diet accelerates the progression of diabetes in Zhx2BKO mice

Ins2-Cre and Zhx2BKO mice were fed an HFD diet for 24 weeks.

(A) Overall appearance of Ins2-Cre and Zhx2BKO mice.

(B) Growth curve was monitored. (n/Ins2-Cre = 5, n/Zhx2BKO = 6).

(C) Fasting blood glucose level. Five-month-old male Ins2-Cre and Zhx2BKO mice fasted for 6–8 h (n/Ins2-Cre = 7, n/Zhx2BKO = 9).

(D) Fasting serum insulin level. Mice were treated in C. (n/Ins2-Cre = 7, n/Zhx2BKO = 9).

(E) IPGTT. Blood glucose levels (left panel) and area under the curve (AUC) (right panel) during the intraperitoneal glucose tolerance test. (n/$Zhx2^{f/f}$ = 5, n/Ins2-Cre = 5, n/Zhx2BKO = 6).

(F) *In vivo* GSIS. Glucose was administered to 16 h fasted mice by intraperitoneal injection, and plasma insulin was measured at the indicated time points. (n/Ins2-Cre = 7, n/Zhx2BKO = 7).

(G) ITT. Mice fasted for 6 h were intraperitoneally injected with a single dose of recombinant human insulin (0.7 U/kg body weight). (n/Ins2-Cre = 8, n/Zhx2BKO = 9).

(H–M) Ins2-Cre and Zhx2BKO mice fed an HFD diet for 24 weeks, and H&E staining was performed in pancreatic tissues (H), followed by measurements of the islet area/pancreatic area ratio (I) and islet size (islet) (J). (n/Ins2-Cre = 6, n/Zhx2BKO = 7). IHC staining was used to detect insulin in pancreatic sections (K), followed by measurements of the β-cell area/pancreatic area ratio (L) and β-cell mass (M). (n/Ins2-Cre = 5, n/Zhx2BKO = 5).

(N) IF staining. Ki67-positive cells in islets were normalized to total insulin-positive cells in the same area. Scale bar, 20 μm. Data were statistically analyzed by Student's *t* test or two-way ANOVA with Dunnett's post hoc test (G). Data are presented as the mean ± SEM. *$p < 0.05$, **$p < 0.01$, ns (no significant difference) by Student's *t* test.

Zhx2 promotes β-cell proliferation and insulin secretion

The Gene Expression Profiling Interactive Analysis database[43] (http://gepia.cancer-pku.cn/) was used to evaluate the role of Zhx2 in islet β-cells, and the results showed a positive correlation between *Zhx2* and proliferation (*Pcna, Akt, Ctnnb1,* and *Myc*) or insulin-related genes (*Pdx1, MafA, Pax6, Sla2a2, Abccb,* and *Kcnj11*) in the healthy human pancreas (Figures S6A–S6C). Consistently, *Zhx2* mRNA level was reduced in starvation status, and restored after serum resupplying in MIN6 cells as evidenced by qRT-PCR, which was similar to insulin-related genes (*Ins1, Pdx1*) (Figure 3A). To examine whether Zhx2 could regulate β-cell functions, we interfered or increased Zhx2 expression in β-cells. As expected, proliferation was decreased in MIN6 cells with Zhx2 knockdown (Figures 3B, 3C, S7A, and S7B). To further verify the requirement for Zhx2 in insulin secretion, we first overexpressed Zhx2 in MIN6 cells and treated them with 2.8 or 25 mM glucose. The results showed that high-glucose-stimulated insulin secretion was significantly increased in Zhx2-overexpressed MIN6 cells (Figures 3D, S7C, and S7D). Then, we isolated primary islets from Zhx2BKO mice and control littermate mice, and the islets were treated with 2.8 or 16.7 mM glucose *in vitro*. The results showed that 16.7 mM glucose-stimulated insulin secretion in islets from Zhx2BKO mice was significantly reduced compared with Ins2-Cre mice (Figure 3E). Next, we detected the effects of Zhx2 in regulating β-cell function-related gene expression. Consistently, the expression of proliferation (*Pcna, Ki67*) and insulin (*Pdx1, MafA, Pax6, and Slc2a2*)-related genes were decreased in MIN6 cells with Zhx2 knockdown (Figure 3F), while both the mRNA and protein levels of these genes were increased in MIN6 cells overexpressing Zhx2 (Figures 3G and 3H). We further detected key β-cell genes in the islets of Zhx2BKO and Ins2-Cre mice at 8–12 weeks. Consistently, these key genes were reduced in the islets of Zhx2BKO mice compared to Ins2-Cre mice (Figures 3I and 3J). The above data demonstrate that Zhx2 regulates β-cell function by promoting β-cell proliferation and insulin-related gene expression.

Zhx2 transcriptionally regulates PAX6 in islet β-cells

Next, we tried to determine the molecular mechanism by which Zhx2 regulates islet β-cells. To identify the direct target of Zhx2, we performed a cluster analysis of Zhx2 target genes in ChIP-sequencing data in ccRCC (clear cell renal cell carcinoma),[12] as well as reported genes downregulated in human T2D (GSE50398)[44] and genes highly expressed in β-cells (GSE80673).[45] As shown in Figure 4A, most genes were specific to only one or two clusters. However, two genes (*PAX6* and *SLC2A2*) were enriched in all three clusters, which are believed to be Zhx2-regulated genes in β-cell function. Several studies have confirmed that Pax6 binds to the promoter regions of several key genes regulating β-cells, such as *SLC2A2*, *Pdx1*, *MafA*, and *INS*.[27,31] Therefore, we hypothesized that Zhx2 might regulate β-cell function in a Pax6-dependent manner. To verify the effects of Zhx2 on Pax6, we detected Pax6 expression in the islets of Zhx2BKO and control mice fed an HFD for 6 months. Both IF and qRT-PCR results showed that Pax6 was significantly reduced in the islets of Zhx2BKO mice after HFD feeding (Figures 4B and 4C). Next, we found that Zhx2 overexpression significantly increased Pax6 expression (Figures 4D and S7E–S7G). In accordance with the effect of Zhx2 on Pax6 expression, a dual luciferase assay demonstrated that Zhx2 overexpression markedly promoted Pax6 promoter activity in MIN6 cells (Figure 4E). We searched the potential unique binding sites of Zhx2 on Pax6 promoter regions,[12] and we found three unique motifs of Zhx2 at

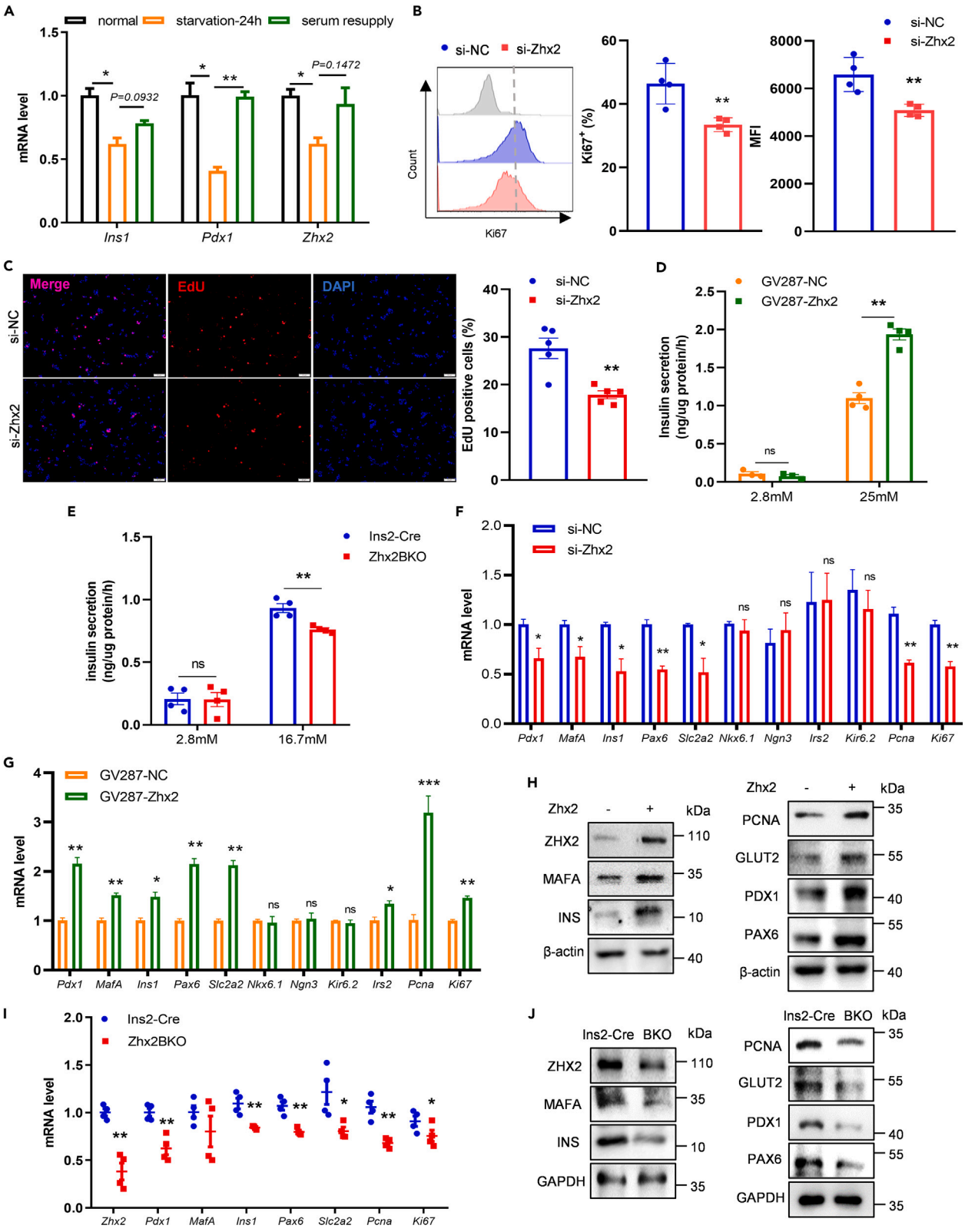
A
normal
starvation-24h
serum resupply
mRNA level
P=0.0932
P=0.1472
Ins1
Pdx1
Zhx2
B
si-NC
si-Zhx2
Count
Ki67
Ki67+ (%)
MFI
C
Merge
EdU
DAPI
si-NC
si-Zhx2
EdU positive cells (%)
D
GV287-NC
GV287-Zhx2
Insulin secretion (ng/ug protein/h)
ns
2.8mM
25mM
E
Ins2-Cre
Zhx2BKO
insulin secretion (ng/ug protein/h)
2.8mM
16.7mM
F
si-NC
si-Zhx2
mRNA level
Pdx1
MafA
Ins1
Pax6
Slc2a2
Nkx6.1
Ngn3
Irs2
Kir6.2
Pcna
Ki67
G
GV287-NC
GV287-Zhx2
mRNA level
H
Zhx2
kDa
ZHX2
MAFA
INS
β-actin
PCNA
GLUT2
PDX1
PAX6
I
Ins2-Cre
Zhx2BKO
mRNA level
J
Ins2-Cre
BKO
GAPDH

Figure 3. Zhx2 promotes β-cell proliferation and insulin-related genes expression

(A) MIN6 cells were starved for 24 h, followed by serum resupply for another 12 h. Total RNA isolated from MIN6 cells in the three groups was subjected to qRT-PCR analysis for the indicated gene expression. mRNA levels were normalized to β-actin mRNA.

(B) MIN6 cells were transfected with si-NC or si-Zhx2 for 72 h. The percentage of MIN6 cell proliferation versus control was measured by flow cytometry. Flow cytometry histograms showing the level of Ki67 in MIN6 cell lines after interference with Zhx2 expression for 72 h (n = 4).

(C) MIN6 cells were silenced for Zhx2 expression for 72 h and subjected to EdU incorporation assays. The new generation cells were detected via EdU (red). DAPI stained nuclei blue. Merged view of EdU (red) and DAPI (blue) showing the overlap (n = 5).

(D) MIN6 cells infected with GV287 (Vector) or GV287-Zhx2 lentiviruses were treated with 2.8 mM or 25 mM glucose. Insulin levels in the culture supernatants were determined by ELISA (n = 4).

(E) Pancreatic islets from 8-week-old Ins2-Cre and Zhx2BKO mice were treated with 2.8 or 16.7 mM glucose. Insulin levels in the culture supernatants were determined by ELISA. (n/Ins2-Cre = 3, n/Zhx2BKO = 3).

(F) Total RNA isolated from si-NC- or si-Zhx2-transfected MIN6 cells was subjected to qRT-PCR analysis for the indicated gene expression. mRNA levels were normalized to β-actin mRNA.

(G–J) MIN6 cells were infected with GV287 (Vector) or GV287-Zhx2 lentiviruses, and qRT-PCR was performed to detect the indicated gene expression. mRNA levels were normalized to β-actin mRNA. MIN6 cells were transfected with pc3.0 or pcZhx2 for 72 h, and Western blotting (H) was performed to detect the expression of the indicated genes. Expression of the indicated genes in islets of Ins2-Cre and Zhx2BKO mice was measured by qRT-PCR (I) or Western blotting (J). mRNA levels were normalized to β-actin mRNA (n/Ins2-Cre = 4, n/Zhx2BKO = 4). Data are presented as the mean ± SEM. *$p < 0.05$, **$p < 0.01$, ***$p < 0.001$, ns (no significant difference) by Student's *t* test.

−79/-70 bp, −766/-758 bp, and −836/-828 bp of *Pax6* (Figure 4F). Furthermore, a ChIP assay was performed with anti-Zhx2, and the results demonstrated that Zhx2 significantly occupied the Pax6 promoter in MIN6 cells (Figures 4G and 4H). All these results suggest that Zhx2 is capable of binding to the Pax6 locus, thereby positively regulating Pax6 transcription.

Zhx2 functions in islet β-cells partially depend on Pax6

To validate the involvement of Pax6 in the Zhx2-mediated regulation of islet β-cell proliferation and function, adenovirus-overexpressing Pax6 or siRNA-targeting Pax6 was included in MIN6 cells and islets. MIN6 cells were transfected with si-NC or si-Zhx2 for 24 h and then infected with Pax6 adenovirus for another 48 h. As expected, proliferation was reversed in Pax6-overexpressing MIN6 cells with Zhx2 deficiency (Figures 5A and S7H). Moreover, high-glucose-stimulated insulin secretion was also reversed in Pax6-overexpressing MIN6 cells (Figure 5B). Consistently, Pax6 overexpression reversed the downregulation of proliferation and insulin-related genes in the Zhx2 knockdown group of MIN6 cells and islets (Figures 5C, 5D, and S7I). In contrast, Pax6 interference reversed the upregulation of proliferation and insulin-related genes in the Zhx2 overexpression group (Figures 5E and 5F). Overall, these data illustrate that Zhx2 promotes β-cell proliferation and function by promoting Pax6 transcription.

DISCUSSION

Recently, Zhx2 has been thoroughly studied in tumor and inflammatory diseases.[3,20,22] Zhx2 regulates the multiple cell proliferation and development of multiple cell types, such as cancer cells, liver cells, nerve cells, red blood cells, and B cells.[12,15–18] We have reported that Zhx2 accelerates sepsis by promoting macrophage glycolysis[22] and restricts NK cell maturation by reducing the IL-15 response and Zeb2 expression.[21] Zhx2 is a double-edged sword in different cancers. On the one hand, Zhx2 promotes cancer progression by acting as a VHL target and regulating its protein stability,[12] activating MEK/ERK signaling,[14] or promoting HIF1α.[20] In contrast, Zhx2 acts as a negative regulator of multiple cancers by repressing the expression of cyclins A and E,[13] targeting and inhibiting the p38MAPK pathway,[46] or suppressing stem cell-like traits through KDM2A-mediated H3K36 demethylation.[19] The above results indicate that Zhx2 regulates a variety of cellular functions, particularly in cell proliferation and inflammation. In this study, high expression of Zhx2 in islet β-cells was identified for the first time, and the diabetic environment reduced Zhx2 expression in islets, which prompted us to further investigate the unknown functions of Zhx2 in islet β-cells and diabetes.

T2D has become a global public health threat and is known to be associated with chronic inflammation.[24,25] β-cell failure and insulin secretion impairment act as major features determining the progression to hyperglycemia and overt T2D. Therefore, understanding the molecular mechanisms maintaining β-cell function or indicating β-cell dysfunction is of paramount importance, which would provide a therapeutic target for diabetes intervention. Here, we initially determined the role of Zhx2 in islet β-cells and T2D, illustrating that islet β-cell-specific Zhx2 deficiency causes β-cell loss and dysfunction in a PAX6-dependent manner. Our results showed that Zhx2 knockout in islet β-cells significantly reduced insulin secretion as well as β-cell

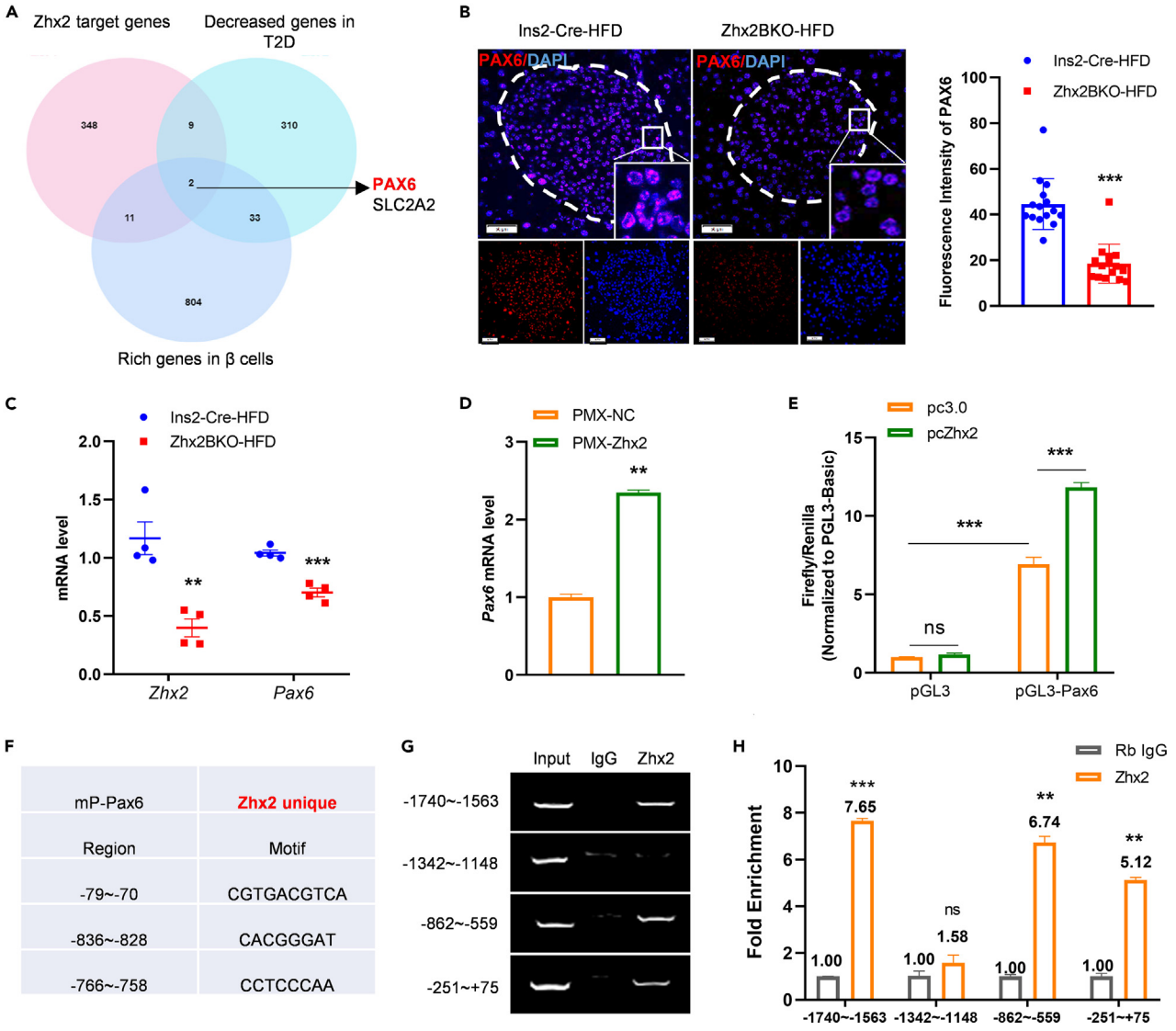

Figure 4. Zhx2 transcriptionally regulates Pax6 in islet β-cells

(A) Zhx2 target genes from ChIP-seq, decreased genes in human T2D ($p < 0.005$ and logFC >0.3) and enriched genes in β-cells (enrichment of the top 1000 expressed genes of three β-cell groups).

(B) IF staining was used to assay Pax6 protein expression (red) in pancreatic tissues of Ins2-Cre and Zhx2BKO mice fed an HFD for 20 weeks; nuclei were stained with DAPI (blue). Scale bar, 20 μm.

(C) Islets from Ins2-Cre and Zhx2BKO mice fed an HFD for 20 weeks were used to detect Pax6 mRNA expression by qRT-PCR analysis. mRNA levels were normalized to β-actin mRNA (n/Ins2-Cre = 4, n/Zhx2BKO = 4).

(D) MIN6 cells infected with PMX (Vector) or PMX-Zhx2 lentiviruses. GFP-positive MIN6 cells were sorted by FACS, and Pax6 expression was analyzed by qRT-PCR. mRNA levels were normalized to β-actin mRNA.

(E) A dual luciferase reporter assay was performed in MIN6 cells co-transfected with the pGL3-Pax6 promoter reporter plasmid and pcZhx2. Relative luciferase activities were normalized as the fold value versus the mock control.

(F–H) The Zhx2 unique motif of the Pax6 promoter region was predicted from sequence alignment. ChIP analysis in MIN6 cells. ChIP analysis was performed using anti-Zhx2 in MIN6 cells. Primers targeting *Pax6* promoter regions were included for PCR (G) and qPCR (H) analysis. Data are presented as the mean ± SEM. **$p < 0.01$, ***$p < 0.001$, ns (no significant difference) by Student's *t* test.

mass in HFD-fed mice, as characterized by their normalized fasting blood glucose levels and glucose tolerance. Importantly, we found that Zhx2 deletion completely caused β-cell loss and dysfunction in T2D mice. By ChIP assay, Zhx2 was found to bind to the PAX6 promoter regions. A dozen of PAX6-targeting genes were also found to be significantly downregulated in islets from Zhx2BKO mice. Thus, our findings suggest that Zhx2 may represent a therapeutic target for T2D prevention and treatment.

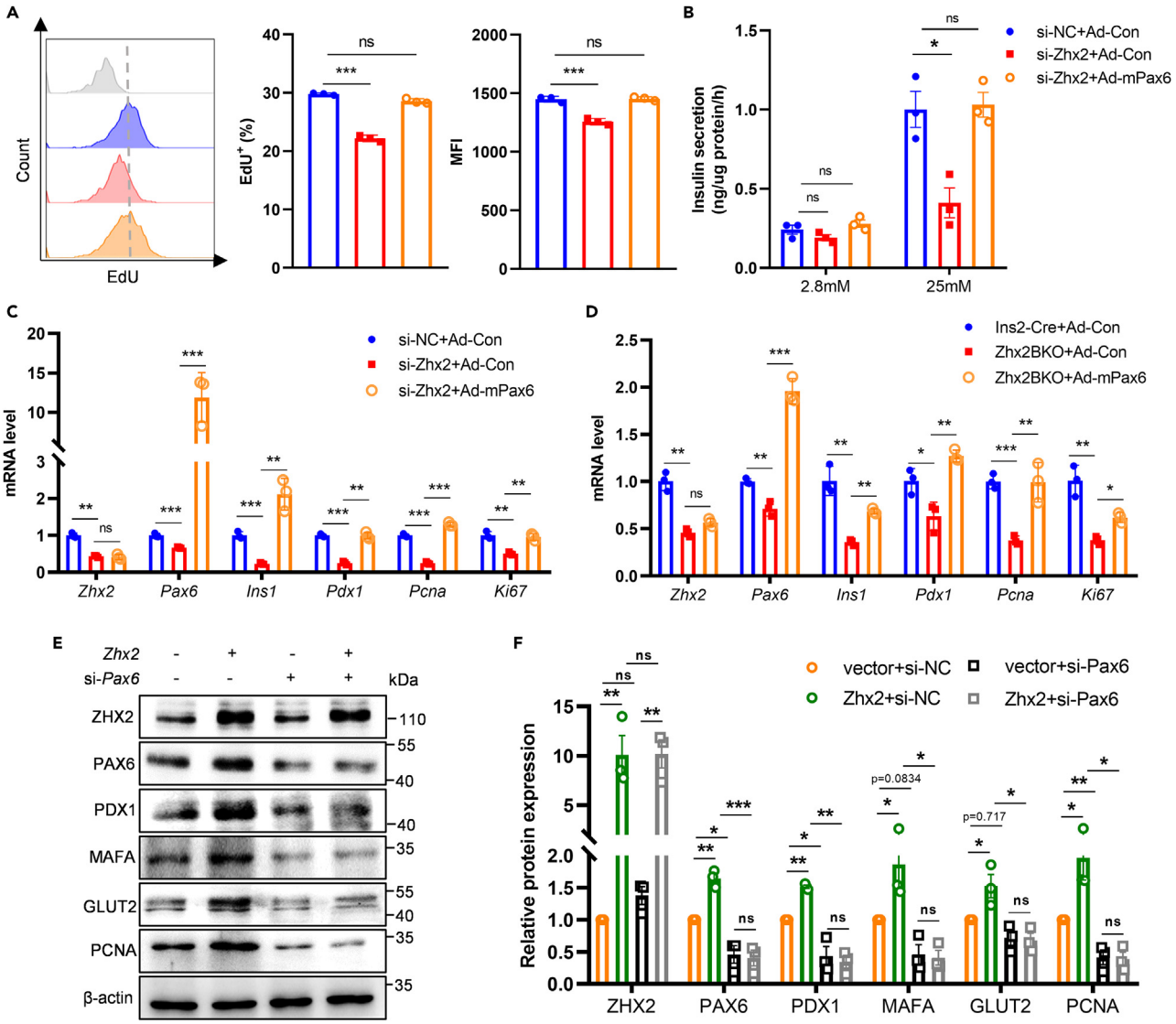

Figure 5. Zhx2 maintains islet β-cell function depending on Pax6

MIN6 cells were transfected with si-NC or si-Zhx2 for 12 h and then infected with Ad-GFP or Ad-mPax6 for 48 h.

(A) The percentage of MIN6 cell proliferation versus control was measured by flow cytometry. Flow cytometry histograms showing the level of EdU in MIN6 cell lines (n = 3).

(B) MIN6 cells were treated with 2.8 or 25 mM glucose. Insulin levels in the culture supernatants were determined by ELISA (n = 3).

(C) qRT-PCR was performed to detect the indicated gene expression. mRNA levels were normalized to β-actin mRNA (n = 3).

(D) Islets were infected with Ad-GFP or Ad-mPax6 for 48 h, and qRT-PCR was performed to detect the indicated gene expression. mRNA levels were normalized to β-actin mRNA (n = 3).

(E) MIN6 cells infected with GV287 (Vector) or GV287-Zhx2 lentiviruses and transfected with si-NC or si-Pax6 for 72 h. Protein levels of these genes were measured by Western blotting.

(F) MIN6 cells were co-transfected with si-NC or si-Pax6 and the pc3.0 or pcZhx2 plasmid for 72 h. The protein levels of these genes were measured by Western blotting and analyzed by ImageJ assay. Data are presented as the mean ± SEM. *p < 0.05, **p < 0.01, ***p < 0.001, ns (no significant difference) by Student's *t* test.

Ins2-Cre (RIP-Cre) has been reported to target Cre expression in certain areas in the hypothalamus.[39] In our study, we detected abnormal glucose tolerance in Ins2-Cre mice compared to $Zhx2^{f/f}$ mice (Figure 1I). This raises the possibility that Zhx2 loss in the hypothalamus might contribute to the diabetic phenotypes of Zhx2BKO mice. However, we observed an extremely low level of Zhx2 protein in the hypothalamus (Figures 1C, S3B, and S3C). Furthermore, the protein levels of Zhx2 were not markedly reduced in the brain or hypothalamus of Zhx2BKO mice relative to Ins2-Cre mice (Figures 1C and S3D). These results suggest

that Ins2-Cre may not target hypothalamus cells with low Zhx2 expression and support the idea that the absence of Zhx2 in islet β-cells but not in the hypothalamus contributes to the diabetic phenotypes displayed by Zhx2BKO mice.

Here, we demonstrate that Zhx2 regulates β-cell function and mass by modulating, at least in part, Pax6. The reduced Pax6 levels suppress β-cell mass and insulin secretion.[30,33,47] Pax6 has been shown to bind the promoter regions of several key β-cell genes, such as *Slc2a2, Pdx1, MafA,* and *Ins*.[27,31] In this study, the protein levels of PAX6-targeting genes (*Pdx1, MafA, Slc2a2, and Ins1*) were found to be significantly downregulated in islets from Zhx2BKO mice. *In vitro*, we confirmed that Pax6 overexpression reversed the downregulation of proliferation and insulin secretion in the Zhx2 knockdown group (Figures 5A–5D). Therefore, we believe that Pax6 plays an important role in Zhx2-mediated regulation of proliferation and insulin secretion in islet β-cells. Of course, the key role of Pax6 should be further verified using a diabetic model *in vivo*. However, we could not exclude the possibility that Zhx2 might directly regulate the expression of *Pdx1, MafA, Ins*, or *Slc2a2*, especially *Slc2a2*, which was also found to be a Zhx2 target gene (Figure 4A). In addition, the results showed that PDX1 protein levels appeared to be much more reduced in islets from Zhx2BKO mice (Figure 3J), indicating that Pdx1 might also be a potential mechanism. Although we observed the binding of Zhx2 to the *Pax6* promoter regions, an electrophoretic mobility shift assay is required to confirm the direct interaction of Zhx2 with *Pax6*. In addition, assay for targeting accessible chromatin with high-throughput sequencing (ATAC-seq) is also needed to clarify whether Zhx2 regulates *Pax6* in a direct way. In addition, recent studies have reported that the dedifferentiation or transdifferentiation of β-cells may lead to diabetes, and α and β-cells can interconvert under certain conditions.[48,49] We found that Zhx2 deletion in islet β-cells led to increased α cells in islets (Figures 1N and S5), indicating that β-cells might transdifferentiate into α cells, which might be another mechanism by which Zhx2 participates in T2D pathogenesis. Therefore, further investigation in the future is required to illustrate the exact mechanism.

In conclusion, our study provides a working model to explain how Zhx2 modulates β-cell function and β-cell mass, therefore contributing to T2D. Emerging studies have reported Pax6 as an indispensable transcription factor controlling GSIS in β-cells.[30,33,34] This study identifies Zhx2 as a key regulator of Pax6 in β-cells, which may provide an approach to help combat diabetes-associated glucose disorders based on its positive role in β-cell function. We further evaluated the role of Zhx2 in protecting β-cell mass and function under diabetic injury. Our work reveals that Zhx2 is essential for β-cell function; therefore, enhancing Zhx2 expression should be helpful to reverse β-cell loss under diabetic conditions.

Limitations of the study

Our results suggest that targeting Zhx2 might provide a novel strategy for diabetes therapy. However, there are still a few limitations in this study. First, with the help of ChIP coupled with qRT-PCR, we confirmed that Zhx2 exerts its function by binding to the promoter of *Pax6*. However, the present results could not demonstrate whether Zhx2 directly binds to the promoter region of downstream targets to transcriptionally modulate gene expression. Therefore, the precise molecular mechanism by which Zhx2 regulates Pax6 expression needs to be further investigated in the future. Second, the results of rescue assays showed that the intervention of Pax6 expression partially restored the promoting effect of Zhx2 on β-cell function in islets. Therefore, there might be other mechanisms contributing to the role of Zhx2 in modulating β-cell function, which needs to be further identified. Finally, our study mainly relied on a series of animal models and lacked clinical samples to verify our results.

STAR★METHODS

Detailed methods are provided in the online version of this paper and include the following:

- KEY RESOURCES TABLE
- RESOURCE AVAILABILITY
  - Lead contact
  - Materials availability
  - Data and code availability
- EXPERIMENTAL MODEL AND SUBJECT DETAILS
  - Mouse models
  - Cell lines and cell culture
  - Viruses

SUPPLEMENTAL INFORMATION

Supplemental information can be found online at https://doi.org/10.1016/j.isci.2023.106871.

ACKNOWLEDGMENTS

Thanks for the supporting from Collaborative Innovation Center of Technology and Equipment for Biological Diagnosis and Therapy in Universities of Shandong, Translational Medicine Core Facility of Advanced Medical Research Institute, Shandong University. We thank Professor Yaoqin Gong (Shandong University) for providing the db/m mice. We thank Professor Ling Gao (ShengLi Hospital of Shandong University) for providing MIN6 cell line. We thank for the National Natural Science Foundation of China (82271878, 81971480, 81970508), Natural Science Foundation of Shandong Province (ZR2019LZL013, ZR2020ZD12), National Key Research and Development Program (2021YFC2300603), and Shandong University multidisciplinary research and innovation team of young scholars (2020QNQT001).

AUTHOR CONTRIBUTIONS

L.D. performed experiments, conducted data analysis, and wrote the manuscript, Y.Z., Yi.W., and Yu.W. performed experiments and data analysis. Z.T., C.C., P.L., and B.W. contributed to discussion. C.M., X.L., Z.W., C.L., and X.Y. gave careful guidance and assistance for this project. L.G. was in charge of study design, data analysis, work organization/supervision, and manuscript review. All authors discussed the results and commented on the manuscript.

DECLARATION OF INTERESTS

The authors have no financial conflicts of interest.

Received: November 18, 2022
Revised: April 5, 2023
Accepted: May 9, 2023
Published: May 13, 2023

REFERENCES

1. Khan, M.A.B., Hashim, M.J., King, J.K., Govender, R.D., Mustafa, H., and Al Kaabi, J. (2020). Epidemiology of type 2 diabetes - global burden of disease and forecasted trends. J. Epidemiol. Glob. Health *10*, 107–111. https://doi.org/10.2991/jegh.k.191028.001.

2. Bellary, S., Kyrou, I., Brown, J.E., and Bailey, C.J. (2021). Type 2 diabetes mellitus in older adults: clinical considerations and management. Nat. Rev. Endocrinol. *17*, 534–548. https://doi.org/10.1038/s41574-021-00512-2.

3. Zhang, Y., Sun, M., Gao, L., Liang, X., Ma, C., Lu, J., and Yue, X. (2022). ZHX2 inhibits thyroid cancer metastasis through transcriptional inhibition of S100A14. Cancer Cell Int. *22*, 76. https://doi.org/10.1186/s12935-022-02499-w.

4. Meier, J.J., Butler, A.E., Saisho, Y., Monchamp, T., Galasso, R., Bhushan, A., Rizza, R.A., and Butler, P.C. (2008). Beta-cell replication is the primary mechanism subserving the postnatal expansion of beta-cell mass in humans. Diabetes *57*, 1584–1594. https://doi.org/10.2337/db07-1369.

5. Christensen, A.A., and Gannon, M. (2019). The beta cell in type 2 diabetes. Curr. Diab. Rep. *19*, 81. https://doi.org/10.1007/s11892-019-1196-4.

6. Rosengren, A.H., Braun, M., Mahdi, T., Andersson, S.A., Travers, M.E., Shigeto, M., Zhang, E., Almgren, P., Ladenvall, C., Axelsson, A.S., et al. (2012). Reduced insulin exocytosis in human pancreatic β-cells with gene variants linked to type 2 diabetes. Diabetes *61*, 1726–1733. https://doi.org/10.2337/db11-1516.

7. Sone, H., and Kagawa, Y. (2005). Pancreatic beta cell senescence contributes to the pathogenesis of type 2 diabetes in high-fat diet-induced diabetic mice. Diabetologia *48*, 58–67. https://doi.org/10.1007/s00125-004-1605-2.

8. Bloomgarden, Z.T. (2008). American college of endocrinology pre-diabetes consensus conference: part three. Diabetes Care *31*, 2404–2409. https://doi.org/10.2337/dc08-zb12.

9. Ahmadi, N., Valizadeh, M., Hadaegh, F., Mahdavi, M., Tasdighi, E., Azizi, F., and Khalili, D. (2021). Metabolic risk factors among prediabetic individuals and the trajectory toward the diabetes incidence. J. Diabetes *13*, 905–914. https://doi.org/10.1111/1753-0407.13205.

10. Maschio, D.A., Oliveira, R.B., Santos, M.R., Carvalho, C.P.F., Barbosa-Sampaio, H.C.L., and Collares-Buzato, C.B. (2016). Activation of the Wnt/β-catenin pathway in pancreatic beta cells during the compensatory islet hyperplasia in prediabetic mice. Biochem. Biophys. Res. Commun. *478*, 1534–1540. https://doi.org/10.1016/j.bbrc.2016.08.146.

11. Kawata, H., Yamada, K., Shou, Z., Mizutani, T., Yazawa, T., Yoshino, M., Sekiguchi, T., Kajitani, T., and Miyamoto, K. (2003). Zinc-fingers and homeoboxes (ZHX) 2, a novel member of the ZHX family, functions as a transcriptional repressor. Biochem. J. *373*, 747–757. https://doi.org/10.1042/bj20030171.

12. Zhang, J., Wu, T., Simon, J., Takada, M., Saito, R., Fan, C., Liu, X.D., Jonasch, E., Xie, L., Chen, X., et al. (2018). VHL substrate transcription factor ZHX2 as an oncogenic driver in clear cell renal cell carcinoma. Science (New York, N.Y.) *361*, 290–295. https://doi.org/10.1126/science.aap8411.

13. Yue, X., Zhang, Z., Liang, X., Gao, L., Zhang, X., Zhao, D., Liu, X., Ma, H., Guo, M., Spear, B.T., et al. (2012). Zinc fingers and homeoboxes 2 inhibits hepatocellular carcinoma cell proliferation and represses expression of cyclins A and E. Gastroenterology *142*, 1559–1570.e2. https://doi.org/10.1053/j.gastro.2012.02.049.

14. Zhu, L., Ding, R., Yan, H., Zhang, J., and Lin, Z. (2020). ZHX2 drives cell growth and migration via activating MEK/ERK signal and induces sunitinib resistance by regulating the autophagy in clear cell renal cell carcinoma. Cell Death Dis. *11*, 337. https://doi.org/10.1038/s41419-020-2541-x.

15. De Andrade, T., Moreira, L., Duarte, A., Lanaro, C., De Albuquerque, D., Saad, S., and Costa, F. (2010). Expression of new red cell-related genes in erythroid differentiation. Biochem. Genet. *48*, 164–171. https://doi.org/10.1007/s10528-009-9310-y.

16. Hystad, M.E., Myklebust, J.H., Bø, T.H., Sivertsen, E.A., Rian, E., Forfang, L., Munthe, E., Rosenwald, A., Chiorazzi, M., Jonassen, I., et al. (2007). Characterization of early stages of human B cell development by gene expression profiling. J. Immunol. *179*, 3662–3671. https://doi.org/10.4049/jimmunol.179.6.3662.

17. Peterson, M.L., Ma, C., and Spear, B.T. (2011). Zhx2 and Zbtb20: novel regulators of postnatal alpha-fetoprotein repression and their potential role in gene reactivation during liver cancer. Semin. Cancer Biol. *21*, 21–27. https://doi.org/10.1016/j.semcancer.2011.01.001.

18. Wu, C., Qiu, R., Wang, J., Zhang, H., Murai, K., and Lu, Q. (2009). ZHX2 interacts with ephrin-B and regulates neural progenitor maintenance in the developing cerebral cortex. J. Neurosci. *29*, 7404–7412. https://doi.org/10.1523/jneurosci.5841-08.2009.

19. Lin, Q., Wu, Z., Yue, X., Yu, X., Wang, Z., Song, X., Xu, L., He, Y., Ge, Y., Tan, S., et al. (2020). ZHX2 restricts hepatocellular carcinoma by suppressing stem cell-like traits through KDM2A-mediated H3K36 demethylation. EBioMedicine *53*, 102676. https://doi.org/10.1016/j.ebiom.2020.102676.

20. Fang, W., Liao, C., Shi, R., Simon, J.M., Ptacek, T.S., Zurlo, G., Ye, Y., Han, L., Fan, C., Bao, L., et al. (2021). ZHX2 promotes HIF1α oncogenic signaling in triple-negative breast cancer. Elife *10*, e70412. https://doi.org/10.7554/eLife.70412.

21. Tan, S., Guo, X., Li, M., Wang, T., Wang, Z., Li, C., Wu, Z., Li, N., Gao, L., Liang, X., and Ma, C. (2021). Transcription factor Zhx2 restricts NK cell maturation and suppresses their antitumor immunity. J. Exp. Med. *218*, e20210009. https://doi.org/10.1084/jem.20210009.

22. Wang, Z., Kong, L., Tan, S., Zhang, Y., Song, X., Wang, T., Lin, Q., Wu, Z., Xiang, P., Li, C., et al. (2020). Zhx2 accelerates sepsis by promoting macrophage glycolysis via Pfkfb3. J. Immunol. *204*, 2232–2241. https://doi.org/10.4049/jimmunol.1901246.

23. Erbilgin, A., Seldin, M.M., Wu, X., Mehrabian, M., Zhou, Z., Qi, H., Dabirian, K.S., Sevag Packard, R.R., Hsieh, W., Bensinger, S.J., et al. (2018). Transcription factor Zhx2 deficiency reduces atherosclerosis and promotes macrophage apoptosis in mice. Arterioscler. Thromb. Vasc. Biol. *38*, 2016–2027. https://doi.org/10.1161/atvbaha.118.311266.

24. Garneau, L., Terada, T., Mistura, M., Mulvihill, E.E., Reed, J.L., and Aguer, C. (2023). Exercise training reduces circulating cytokines in male patients with coronary artery disease and type 2 diabetes: a pilot study. Physiol. Rep. *11*, e15634. https://doi.org/10.14814/phy2.15634.

25. Sater, M.S., AlDehaini, D.M.B., Malalla, Z.H.A., Ali, M.E., and Giha, H.A. (2023). Plasma IL-6, TREM1, uPAR, and IL6/IL8 biomarkers increment further witnessing the chronic inflammation in type 2 diabetes. Horm. Mol. Biol. Clin. Investig. https://doi.org/10.1515/hmbci-2022-0103.

26. Wu, H., Liu, Y., Wang, H., and Xu, X. (2015). High-fat diet induced insulin resistance in pregnant rats through pancreatic pax6 signaling pathway. Int. J. Clin. Exp. Pathol. *8*, 5196–5202.

27. Gosmain, Y., Katz, L.S., Masson, M.H., Cheyssac, C., Poisson, C., and Philippe, J. (2012). Pax6 is crucial for beta-cell function, insulin biosynthesis, and glucose-induced insulin secretion. Mol. Endocrinol. *26*, 696–709. https://doi.org/10.1210/me.2011-1256.

28. Sander, M., Neubüser, A., Kalamaras, J., Ee, H.C., Martin, G.R., and German, M.S. (1997). Genetic analysis reveals that PAX6 is required for normal transcription of pancreatic hormone genes and islet development. Genes Dev. *11*, 1662–1673. https://doi.org/10.1101/gad.11.13.1662.

29. Panneerselvam, A., Kannan, A., Mariajoseph-Antony, L.F., and Prahalathan, C. (2019). PAX proteins and their role in pancreas. Diabetes Res. Clin. Pract. *155*, 107792. https://doi.org/10.1016/j.diabres.2019.107792.

30. So, W.Y., Liu, W.N., Teo, A.K.K., Rutter, G.A., and Han, W. (2021). Paired box 6 programs essential exocytotic genes in the regulation of glucose-stimulated insulin secretion and glucose homeostasis. Sci. Transl. Med. *13*, eabb1038. https://doi.org/10.1126/scitranslmed.abb1038.

31. Gosmain, Y., Marthinet, E., Cheyssac, C., Guérardel, A., Mamin, A., Katz, L.S., Bouzakri, K., and Philippe, J. (2010). Pax6 controls the expression of critical genes involved in pancreatic {alpha} cell differentiation and function. J. Biol. Chem. *285*, 33381–33393. https://doi.org/10.1074/jbc.M110.147215.

32. Chen, Y., Feng, R., Wang, H., Wei, R., Yang, J., Wang, L., Wang, H., Zhang, L., Hong, T.P., and Wen, J. (2014). High-fat diet induces early-onset diabetes in heterozygous Pax6 mutant mice. Diabetes Metabol. Res. Rev. *30*, 467–475. https://doi.org/10.1002/dmrr.2572.

33. Sheng, J., Wang, L., Tang, P.M.K., Wang, H.L., Li, J.C., Xu, B.H., Xue, V.W., Tan, R.Z., Jin, N., Chan, T.F., et al. (2021). Smad3 deficiency promotes beta cell proliferation and function in db/db mice via restoring Pax6 expression. Theranostics *11*, 2845–2859. https://doi.org/10.7150/thno.51857.

34. Swisa, A., Avrahami, D., Eden, N., Zhang, J., Feleke, E., Dahan, T., Cohen-Tayar, Y., Stolovich-Rain, M., Kaestner, K.H., Glaser, B., et al. (2017). PAX6 maintains β cell identity by repressing genes of alternative islet cell types. J. Clin. Invest. *127*, 230–243. https://doi.org/10.1172/jci88015.

35. Srinivasan, K., Viswanad, B., Asrat, L., Kaul, C.L., and Ramarao, P. (2005). Combination of high-fat diet-fed and low-dose streptozotocin-treated rat: a model for type 2 diabetes and pharmacological screening. Pharmacol. Res. *52*, 313–320. https://doi.org/10.1016/j.phrs.2005.05.004.

36. Zhu, K., Lai, Y., Cao, H., Bai, X., Liu, C., Yan, Q., Ma, L., Chen, D., Kanaporis, G., Wang, J., et al. (2020). Kindlin-2 modulates MafA and β-catenin expression to regulate β-cell function and mass in mice. Nat. Commun. *11*, 484. https://doi.org/10.1038/s41467-019-14186-y.

37. Ahmed Abdalhamid Osman, M., Sun, Y.J., Li, R.J., Lin, H., Zeng, D.M., Chen, X.Y., He, D., Feng, H.W., Yang, Z., Wang, J., et al. (2019). Deletion of pancreatic β-cell adenosine kinase improves glucose homeostasis in

young mice and ameliorates streptozotocin-induced hyperglycaemia. J. Cell Mol. Med. *23*, 4653–4665. https://doi.org/10.1111/jcmm.14216.

38. Magnuson, M.A., and Osipovich, A.B. (2013). Pancreas-specific Cre driver lines and considerations for their prudent use. Cell Metab. *18*, 9–20. https://doi.org/10.1016/j.cmet.2013.06.011.

39. Wicksteed, B., Brissova, M., Yan, W., Opland, D.M., Plank, J.L., Reinert, R.B., Dickson, L.M., Tamarina, N.A., Philipson, L.H., Shostak, A., et al. (2010). Conditional gene targeting in mouse pancreatic ß-Cells: analysis of ectopic Cre transgene expression in the brain. Diabetes *59*, 3090–3098. https://doi.org/10.2337/db10-0624.

40. Heydemann, A. (2016). An overview of murine high fat diet as a model for type 2 diabetes mellitus. J. Diabetes Res. *2016*, 2902351. https://doi.org/10.1155/2016/2902351.

41. Stamateris, R.E., Sharma, R.B., Hollern, D.A., and Alonso, L.C. (2013). Adaptive beta-cell proliferation increases early in high-fat feeding in mice, concurrent with metabolic changes, with induction of islet cyclin D2 expression. Am. J. Physiol. Endocrinol. Metab. *305*, E149–E159. https://doi.org/10.1152/ajpendo.00040.2013.

42. Finegood, D.T., McArthur, M.D., Kojwang, D., Thomas, M.J., Topp, B.G., Leonard, T., and Buckingham, R.E. (2001). Beta-cell mass dynamics in Zucker diabetic fatty rats. Rosiglitazone prevents the rise in net cell death. Diabetes *50*, 1021–1029. https://doi.org/10.2337/diabetes.50.5.1021.

43. Tang, Z., Li, C., Kang, B., Gao, G., Li, C., and Zhang, Z. (2017). GEPIA: a web server for cancer and normal gene expression profiling and interactive analyses. Nucleic Acids Res. *45*, 98–102. https://doi.org/10.1093/nar/gkx247.

44. Fadista, J., Vikman, P., Laakso, E.O., Mollet, I.G., Esguerra, J.L., Taneera, J., Storm, P., Osmark, P., Ladenvall, C., Prasad, R.B., et al. (2014). Global genomic and transcriptomic analysis of human pancreatic islets reveals novel genes influencing glucose metabolism. Proc. Natl. Acad. Sci. USA *111*, 13924–13929. https://doi.org/10.1073/pnas.1402665111.

45. DiGruccio, M.R., Mawla, A.M., Donaldson, C.J., Noguchi, G.M., Vaughan, J., Cowing-Zitron, C., van der Meulen, T., and Huising, M.O. (2016). Comprehensive alpha, beta and delta cell transcriptomes reveal that ghrelin selectively activates delta cells and promotes somatostatin release from pancreatic islets. Mol. Metab. *5*, 449–458. https://doi.org/10.1016/j.molmet.2016.04.007.

46. Tian, X., Wang, Y., Li, S., Yue, W., and Tian, H. (2020). ZHX2 inhibits proliferation and promotes apoptosis of human lung cancer cells through targeting p38MAPK pathway. Cancer Biomark. *27*, 75–84. https://doi.org/10.3233/cbm-190514.

47. Mitchell, R.K., Nguyen-Tu, M.S., Chabosseau, P., Callingham, R.M., Pullen, T.J., Cheung, R., Leclerc, I., Hodson, D.J., and Rutter, G.A. (2017). The transcription factor Pax6 is required for pancreatic β cell identity, glucose-regulated ATP synthesis, and Ca(2+) dynamics in adult mice. J. Biol. Chem. *292*, 8892–8906. https://doi.org/10.1074/jbc.M117.784629.

48. Efrat, S. (2019). Beta-cell dedifferentiation in type 2 diabetes: concise review. Stem Cells (Dayton, Ohio) *37*, 1267–1272. https://doi.org/10.1002/stem.3059.

49. Dor, Y., and Glaser, B. (2013). β-cell dedifferentiation and type 2 diabetes. N. Engl. J. Med. *368*, 572–573. https://doi.org/10.1056/NEJMcibr1214034.

50. De Jesus, D.F., Zhang, Z., Kahraman, S., Brown, N.K., Chen, M., Hu, J., Gupta, M.K., He, C., and Kulkarni, R.N. (2019). m(6)A mRNA methylation regulates human β-cell biology in physiological states and in type 2 diabetes. Nat. Metab. *1*, 765–774. https://doi.org/10.1038/s42255-019-0089-9.

51. Smelt, M.J., Faas, M.M., de Haan, B.J., and de Vos, P. (2008). Pancreatic beta-cell purification by altering FAD and NAD(P)H metabolism. Exp. Diabetes Res. *2008*, 165360. https://doi.org/10.1155/2008/165360.

STAR★METHODS

KEY RESOURCES TABLE

REAGENT or RESOURCE	SOURCE	IDENTIFIER
Antibodies		
GAPDH	Proteintech	Cat# 60004-1-Ig; RRID: AB_2107436
β-actin	Proteintech	Cat# 66009-1-Ig; RRID: AB_2687938
Insulin	Abcam	Cat# ab7842; RRID: AB_306130
Insulin	Santa Cruz Biotechnology	Cat# sc-377071; RRID: AB_2800506
Glucagon	Santa Cruz Biotechnology	Cat# sc-514592; RRID: AB_2629431
Somatostatin	Santa Cruz Biotechnology	Cat# sc-74556; RRID: AB_2271061
ZHX2	Proteintech	Cat# 20136-1-AP
PAX6	Santa Cruz Biotechnology	Cat# sc-81649; RRID: AB_1127044
PDX1	Santa Cruz Biotechnology	Cat# sc-390792; RRID: AB_2313773
MAFA	Santa Cruz Biotechnology	Cat# sc-390491; RRID: AB_2313773
HA-tag	MBL	Cat# M180-3; RRID: AB_10951811
GLUT2	Santa Cruz Biotechnology	Cat# sc-518022; RRID: AB_2890904
PCNA	PCNA	Cat# ab92552; RRID: AB_10561973
Ki67	Abcam	Cat# ab16667; RRID: AB_302459
PE anti-mouse Ki67	eBioscience	Cat# 12-5698-82; RRID: AB_2313773
Rabbit Anti-Goat IgG H&L (HRP)	Proteintech	Cat# SA00001-2; RRID: AB_2722564
Mouse Anti-Goat IgG H&L (HRP)	Proteintech	Cat# SA00001-1; RRID: AB_2722565
Alexa Fluor 594 goat anti-guinea pig IgG	Abcam	Cat# ab150188; RRID: AB_2905555
Alexa Fluor 594 goat anti-mouse IgG	Proteintech	Cat# SA00006-3; RRID: AB_2752247
Alexa Fluor 488 goat anti-rabbit IgG	Proteintech	Cat# SA00006-2; RRID: AB_2651036
Normal Rabbit IgG	Santa Cruz Biotechnology	Cat# sc-2027; RRID: AB_737197
Bacterial and virus strains		
Adenovirus (Ad-mPax6)	WZ Biosciences Inc. China	N/A
Lentiviral (PMX-Zhx2/GV287-Zhx2)	This paper	N/A
Chemicals, peptides, and recombinant proteins		
Dulbecco's modified Eagle's medium (DMEM)	Gibco	Cat# C11995500CP
KRBH buffer	Ybio Biotechnology	Cat# YB6650
DAPI	Beyotime Biotechnology	Cat# C1002
Opti-MEM	Gibco	Cat# 11058–021
Penicillin-Streptomycin	Solarbio	Cat# P1400
DNase	Thermo Fisher	Cat# EN0521
Trypsin-EDTA (0.25%)	Gibco	Cat# 25200072
FBS (fetal bovine serum)	Gibco	Cat# 10091148
Lipofectamine 2000	Invitrogen	Cat# 11668–019
Protein A/G magnetic beads	Bimake	Cat# B23201
TRNzol	TIANGEN	Cat# DP424
ChamQ Universal SYBR® qPCR Master Mix	Vazyme Biotech	Cat# Q711
Anti-Fade Fluorescence Mounting Medium	Abcam	Cat# ab104135
Albumin bovine serum	Solarbio	Cat# A8010
RIPA Lysis Buffer	Beyotime Biotechnology	Cat# P0013D

(*Continued on next page*)

Continued

REAGENT or RESOURCE	SOURCE	IDENTIFIER
PMSF	Beyotime Biotechnology	Cat# ST506
SDS-PAGE loading buffer	Beyotime Biotechnology	Cat# P0015L
Immobilon®-P PVDF membrane	Millipore	Cat# IPVH00010
Insulin	Solarbio	Cat# I8830
Collagenase type V	Solarbio	Cat# C8170,
60% high-fat diet	Research Diets	Cat# D12492
Triton X-100	Solarbio	Cat# T8200
Critical commercial assays		
Mouse Insulin ELISA kit	Elabscience	Cat# E-EL-M1382c
Mouse Insulin ELISA kit	Novus biologicals	Cat# NBP2-62853
EnVision+System-HRP (DAB) kit	Dako North America Inc	Cat# K5007
BeyoClick™ EdU-594	Beyotime Biotechnology	Cat# C0078L
Dual Luciferase Reporter Assay	Promega	Cat# E1960
BCA assay	Beyotime Biotechnology	Cat# P0009
RevertAid First Strand	Thermo Fisher	Cat# K1622
EZMagna ChIP™ A/G Chromatin Immunoprecipitation Kit	Millipore	Cat# 17-10086
Experimental models: Cell lines		
MIN6	Prof. Ling Gao (ShengLi Hospital, China)	N/A
Hepa1-6	ATCC	CRL-1830
EL4	ATCC	TIB-39
CT26	ATCC	CRL-2638
betaTC-6	Prof. Xiangdong Wang (Shandong University, China)	N/A
Experimental models: Organisms/strains		
C57BL/6 wild-type mice	Vital River Laboratory Animal Technology	N/A
Ins2-Cre mice	Jackson Laboratory	Stock No.003573
Zhx2-floxed mice	Prof. B. T. Spear (University of Kentucky)	N/A
db/m mice	Prof. Yaoqin Gong (Shandong University, China)	N/A
Oligonucleotides		
For primers sequence for qPCR see Table S1	This paper	N/A
si-Zhx2:5′- CCGCUGAAUACUACCAAAUTT -3′	GenePharma	N/A
si-Pax6: 5′- GGACCCAUUAUCCAGAUGUTT -3′	GenePharma	N/A
Recombinant DNA		
pcDNA3.0-Zhx2	This paper	N/A
pGL3-Pax6	This paper	N/A
Software and algorithms		
GraphPad Prism version 8.0	GraphPad Software Inc	www.graphpad.com
ZEN 2.3 lite	Carl Zeiss	www.zeiss.com
CytExpert	Beckman	www.beckman.com
FlowJo-V10	BD Biosciences	www.flowjo.com
Snapgene 3.2.1	Snapgene software	www.snapgene.com
ImageJ	software	www.imagej.net
BioRender	software	app. Biorender.com

RESOURCE AVAILABILITY

Lead contact

Further information and requests for resources and reagents should be directed to and will be fulfilled by the lead contact, Lifen Gao (glfflg@sdu.edu.cn).

Materials availability

This study did not generate new unique reagents.

Data and code availability

- This paper does not report original code.
- Any additional information required to reanalyze the data reported in this paper is available from the lead contact upon request.

EXPERIMENTAL MODEL AND SUBJECT DETAILS

Mouse models

Wild-type (WT) C57BL/6 male mice were provided by Shandong University Experimental Animal Center (Jinan, China). Ins2-Cre (RIP-Cre) mice (Stock No. 003573) were purchased from Jackson Laboratory. Zhx2-floxed ($Zhx2^{f/f}$) mice were gifted by Prof. B. T. Spear from the University of Kentucky. To delete Zhx2 in β cells, we bred $Zhx2^{f/f}$ mice with Ins2-Cre mice and generated mice with conditional knockout of Zhx2 in islet β cells ($Ins2^{Cre+/-}$-$Zhx2^{f/f}$ or Zhx2BKO). Ins2-Cre mice were used as controls in this study. After 1 week of diet adaptation, 4- to 6-week-old mice were fed a high-fat diet (HFD; 60% Kcal fat) for 16-24 weeks to induce obesity. db/m mice were provided by Prof. Yaoqin Gong at Shandong University, China. Zhx2BKO mice on the C57BL/6J background were intercrossed to generate double mutations of Zhx2 and Lepr (Zhx2BKO-db/db) or control littermates (Ins2-Cre-db/db). All animal procedures were performed in accordance with the guidelines for the Care and Use of Laboratory Animals of Shandong University, and experiments were performed with the approval of the Animal Ethics Committee of Shandong University (Accreditation number: ECSBMSSDU2019-2-028). WT mice and the T2D model, which were fed a HFD combined with streptozotocin (STZ), were randomly divided into two groups: the control group (four mice) and the STZ + HFD group (four mice). The mice in the control group were fed a normal chow diet (NCD) for 5 months. Mice in the STZ + HFD group were fed a HFD diet at the age of 4 weeks for 1 month, and then mice were fasted for 12 h and intraperitoneally injected with 50 mg/kg STZ (Sigma) for 3 days, followed by HFD-diet feeding for an additional 4 months.

Cell lines and cell culture

The MIN6 cell line was obtained from ShengLi Hospital of Shandong University and cultured in DMEM (Gibco) supplemented with 25 mmol/l glucose, 15% FBS (Gibco), 2.5 mmol/l L-glutamine, 50 mmol/l β-mercaptoethanol, 100 U/ml penicillin and 100 mg/ml streptomycin. Hepa1-6 and EL4 cell lines were initially obtained from the American Type Culture Collection (ATCC, USA) and cultured in DMEM (Gibco) with 10% fetal bovine serum (FBS, Gibco). CT26 cell line was initially obtained from the American Type Culture Collection (ATCC, USA) and cultured in RPMI-1640 medium (Gibco) with 10% fetal bovine serum (FBS). The betaTC-6 cell line was provided by Prof. Xiangdong Wang at Shandong University (China) and cultured in RPMI-1640 medium with 10% FBS.

Viruses

- The lentiviral viruses (PMX-Zhx2/GV287-Zhx2) encoding murine Zhx2 were generated by cloning the corresponding cDNA sequences into the PMX/GV287 vector.
- Adenovirus overexpressing murine Pax6 (Ad-mPax6) under the control of the CMV promoter was designed and supplied by WZ Biosciences Inc., China.

METHOD DETAILS

Islet cells isolation and culture

Pancreas islets were isolated by digestion with 1 mg/ml collagenase type V (Solarbio, China). After digestion at 37°C for 30 min, the islets were dispersed. We separated islets by manually picking them in D-Hank's buffered saline solution. After picking at least twice, the islets were collected and transferred to RPMI 1640

medium supplemented with 10% FBS. The islets were cultured at 37°C in a humidified atmosphere consisting of 5% CO2 and 95% air for 12 h.

β-cells sorting

Mouse islets from C57BL/6 mice were dispersed by treatment with a solution of 1 mg /ml trypsin (Gibco) and 30 μg/ml DNase (Thermo) followed by incubation for 15 min in a 37°C incubator. During digestion, the islets were vortexed every 5 min for 10 s. Then, cold media containing serum was added to stop the digestion, and the cells were washed twice in D-PBS containing 1% fatty-acid-free bovine serum albumin (BSA, Solarbio). β cells were separated from non β cells by autofluorescence-activated[31,50,51] sorting using a FACStar-Plus cell sorter (BD Bioscience).

Fasting-refeeding model

MIN6 cells were cultured in DMEM (Gibco) supplemented with 15% FBS (Gibco) until starvation and serum resupplying treatment started. For the starvation group, MIN6 cells were fasted for 24 h. For the serum re-supplying group, MIN6 cells were fasted for 12 h, and then serum was resupplied for 12 h.

Transfection and infection

pcDNA3.0-Zhx2-HA (pcZhx2) plasmid was constructed as described previously.[18] For transfection, MIN6 cells were plated on 35-mm dishes at a density of 2 $\times 10^5$ cells/cm^2. Twenty-four hours later, the cells were transfected with pcZhx2 or control vector pcDNA3.0 (pc3.0) using Lipofectamine 2000 reagent according to the manufacturer's instructions.

For Zhx2 or Pax6 knockdown, MIN6 cells were transfected with the respective 50 nM siRNA mixture using Lipofectamine 2000 reagent (Invitrogen, USA) for 72 h. The sequences of all siRNA sequence are listed key resources table. The same concentration of scrambled siRNA was used as a negative control.

For lentiviral infection, MIN6 cells were cultured in basal growth medium until 70% confluence, and then replaced with fresh medium containing lentivirus for 16-24 h. After infection, screening was performed in the presence of 10 μg/ml puromycin.

For adenovirus infection, MIN6 cells were cultured in complete DMEM at 1 × 10^6 cells well^{-1} in 12-well plates, and 1 × 10^{10} pfu viruses were added to the plate. After 12 h, culture media were replaced with fresh complete DMEM, and the cells were cultured for another 24–48 h. Islets were cultured in complete DMEM at ~30 islets/well on a 96-well plate, and 1 × 10^8 pfu viruses were added to the plate. After 12 h, the culture media were replaced with fresh complete DMEM, and the islets were cultured for 24–48 h.

Glucose tolerance test (GTT), glucose-stimulated insulin secretion (GSIS) and insulin tolerance test (ITT) *in vivo*

Ins2-Cre, Zhx2$^{f/f}$ and Zhx2BKO (Ins2$^{cre+/-}$Zhx2$^{f/f}$) mice fed a NCD or HFD or Ins2-Cre-db/db and Zhx2BKO-db/db mice were included for GTT, GSIS or ITT assays as described below. For GTT, mice were fasted overnight for 16 h and were given 2 g glucose/kg body weight *via* intraperitoneal injection. Blood glucose levels were determined at 0, 15, 30, 60, 90 and 120 minutes after glucose administration by a glucose meter (Yicheng, China). For GSIS, mice were fasted for 16 h and injected intraperitoneally with 2 g glucose/kg body weight. Blood insulin levels were measured using a murine insulin ELISA kit (Elabscience, China) at the indicated time points after glucose injection. For ITT, mice were fasted for 4-6 h and were intraperitoneally challenged with human insulin (Solarbio) at 0.7 U/kg body weight. Blood glucose levels were subsequently monitored at 0, 15, 30, and 60 min after insulin injection.

Glucose-stimulated insulin secretion (GSIS) *in vitro*

Mouse pancreatic islets (30 islets/well in a 48-well plate) were cultured in 2.5 mM glucose overnight. Thereafter, the islets were washed and incubated for 1 h at 37°C in modified Krebs-Ringer bicarbonate HEPES buffer (KRBH buffer) supplemented with 0.2% bovine serum albumin (BSA) and 2.5 mM glucose. Then, the islets were subjected to treatment with 2.8 mM or 16.7 mM glucose for 1 h at 37°C. The insulin levels were measured with a Mouse Insulin ELISA kit (Novus biologicals) following the manufacturer's instructions. The amount of insulin secretion was normalized to the total cellular protein content.

MIN6 cells (2 ×10^5 cells/well in a 48-well plate) were preincubated overnight in KRBH buffer containing 0.2% BSA supplemented with 2.5 mM glucose and 10% FBS. Then, the cells were washed and incubated for 2 h in 2.8 mM or 25 mM glucose. The insulin levels were measured by a mouse insulin ELISA kit (Elabscience, China) according to the manufacturer's instructions. The amount of insulin secretion was normalized to the total cellular protein content.

Immunohistochemical (IHC) and immunofluorescence (IF) staining

Pancreatic tissues were fixed in 4% paraformaldehyde and embedded in paraffin. For IHC, 5-μm sections were stained with antibodies or control IgG using the EnVision+System-HRP (DAB) kit (Dako North America Inc, USA) according to the manufacturer's instructions. For IF, tissues were incubated with antibodies against insulin (Abcam; Santa Cruz Biotechnology), glucagon (Santa Cruz Biotechnology), somatostatin (Santa Cruz Biotechnology), Zhx2 (Proteintech), PAX6 (Santa Cruz Biotechnology), and Ki67 (Abcam) overnight at 4°C and incubated with antibodies against Alexa Fluor 594 goat anti-guinea pig IgG (Abcam), Alexa Fluor 594 goat anti-mouse IgG (Proteintech), and Alexa Fluor 488 goat anti-rabbit IgG (Proteintech) for 1 h at 37°C. Microscopy analysis was performed with an Olympus IX51 microscope and ImageJ software.

β-cell area and mass measurement

Pancreatic sections were subjected to immunohistochemical or immunofluorescence staining for insulin. Pancreatic sections were imaged using a light microscope (OLYMPUS). The insulin-positive area and pancreatic area were measured using Image J software. The islet β-cell mass was examined using the following equation: total insulin-positive area divided by total pancreatic area, multiplied by pancreas tissue weight.

Western blotting

Lysates of cells or tissues were prepared with RIPA buffer (Beyotime Biotechnology, China). Equal amounts (20-30 μg) were subjected to SDS–PAGE and transferred onto a polyvinylidene difluoride (PVDF) membrane filter. After incubation with the appropriate antibodies against ZHX2 (Proteintech), PCNA (Abcam), PAX6 (Santa Cruz Biotechnology), MAFA (Santa Cruz Biotechnology), PDX1 (Santa Cruz Biotechnology), insulin (Santa Cruz Biotechnology), GLUT2 (Santa Cruz Biotechnology), HA (MBL), β-actin (Proteintech), and GAPDH (Proteintech), secondary antibodies against rabbit IgG (Proteintech) and mouse IgG (Proteintech) were incubated.

Quantitative RT-PCR (qRT-PCR)

Total RNA was extracted from the pancreatic islets or other organs, including the brain, heart, lung, liver, spleen, and fat (white adipose) of mice, MIN6 beta cells and other cell lines (βTC-6, EL4, CT26, Hepa1-6) using TRIzol reagent (Invitrogen). cDNA was synthesized with a RevertAid First Strand cDNA Synthesis Kit (Thermo Fisher Scientific). Real-time quantitative PCR (qPCR) was performed with SYBR Green PCR reagents (TIANGE). The relative mRNA level of the target gene was calculated using the $2^{(-\Delta\Delta Ct)}$ method. The ΔCt was computed with normalization to β-actin, which served as the internal control. The sequences of all the primers are listed in Table S1.

Chromatin immunoprecipitation (ChIP) assay

MIN6 cells transfected with pcZhx2 were collected for ChIP assays using the EZMagna ChIP™ A/G Chromatin Immunoprecipitation Kit (Millipor, Germany) according to the manufacturer's instructions. Cells were fixed and sonicated to shear DNA to 200∼1000 bp and then incubated with the following immunoprecipitating antibodies: anti-Zhx2 antibody (Proteintech) and rabbit IgG (Santa Cruz Biotechnology). As controls, 1/50th of the starting chromatin (Input) was used. The primer sequences of Pax6-promoter Sections are listed in Table S1.

Luciferase reporter assay

The promoter region of the mouse Pax6 gene (-2000 bp ∼ +200 bp) was cloned into the pGL3-Basic vector. The Renilla luciferase plasmid (pRL-TK) was described previously. The firefly luciferase reporter pGL3-Pax6 vector and Renilla luciferase plasmid (pRL-TK) were transiently co-transfected into MIN6 cells with pc3.0 or pcZhx2 plasmids using Lipofectamine 2000 transfection reagent (Invitrogen, USA) according to the instructions. pRL-TK was used to normalize the transfection efficiency. At 8 h post-transfection, fresh medium was

replaced. Twenty-four to 48 h later, luciferase activities were measured by using the dual luciferase reporter assay kit (Promega).

QUANTIFICATION AND STATISTICAL ANALYSIS

Statistical analysis was performed using GraphPad Prism 8.0. Two-tailed unpaired or paired Student's *t* tests between two groups and two-way ANOVA across multiple groups were used to determine significance. Western blotting images are representative of at least three independent experiments. qRT-PCR was performed in triplicate, and each experiment was repeated 2-3 times. All data in the figures are presented as the mean ± SEM (standard error of the mean). Statistical significance was reported as *, $P < 0.05$; **, $P < 0.01$; ***, $P < 0.001$; and n.s., no significance.